Eur. Phys. J. B **43**, 339–345 (2005)
DOI: 10.1140/epjb/e2005-00061-3

THE EUROPEAN PHYSICAL JOURNAL B

Polaron properties in ternary group-III nitride mixed crystals

Z.W. Yan[1,2,a], S.L. Ban[2], and X.X. Liang[2]

[1] CCAST (World Laboratory), P.O. BOX 8730, Beijing 100080, P.R. China
and
College of Science, Inner Mongolia Agricultural University, Hohhot 010018, P.R. China
[2] Department of Physics, Inner Mongolia University, Hohhot 010021, P.R. China

Received 22 October 2004 / Received in final form 10 December 2004
Published online 15 March 2005 –

Abstract. Polaron properties are studied in bulk wurtzite nitride ternary mixed crystals $A_xB_{1-x}N$ (A, B = Al, Ga, In) with the use of a dielectric continuum Fröhlich-like electron-phonon interaction Hamiltonian. The polaronic self-trapping energy and effective mass are analytically derived by taking the mixing properties of the LO and TO polarizations due to the anisotropy effect into account in the mono-phonon approximation. The numerical computation has been performed for the wurtzite ternary mixed crystal materials $In_xGa_{1-x}N$, $Al_xGa_{1-x}N$, and $Al_xIn_{1-x}N$ as functions of the composition x. The results show that the polaronic self-trapping energies in the wurtzite structures are bigger than that in zinc-blende structures for the materials calculated. It is also found that the structure anisotropy increases the electron-phonon interaction in wurtizte nitride semiconductors. The results indicate that the LO-like phonon influence on the polaronic self-trapping energy and effective mass is dominant, and the anisotropy effect is obvious.

PACS. 63.20.Kr Electron-phonon interaction – 71.38.-k Polaron – 78.30.Fs Semiconductor

1 Introduction

Recently, III-nitride (III-N) semiconductors have become important materials for the fabrication of optoelectronic devices operating in the green, blue, and ultraviolet spectral region [1–3]. Much attention has been focused on III-N ternary mixed crystals (TMCs) such as $In_xGa_{1-x}N$, $Al_xGa_{1-x}N$, and $Al_xIn_{1-x}N$ [4–6]. It has been shown that the III-N TMCs are polar semiconductors with a direct band gap over the range of 2.0 eV in InN to 6.3 eV in AlN with an intermediate value 3.5 eV for GaN in a wide range of the composition [2,5]. The III-N TMCs offer more flexible choices for consecutive layers in heterostructures and quantum wells with desirable lattice constants and band offsets, which allows for important potential application of III-nitrides in light-emitting diodes and laser diodes with wavelengths from red to deep ultraviolet. Phonon modes in III-N TMCs $A_xB_{1-x}N$ have been investigated theoretically within the modified random-element isodisplacement (MREI) model [4,5]. In alloy systems one important phenomenon is the mode behavior of the long-wavelength optical phonons. TMCs $A_xB_{1-x}C$ with fully pronounced random alloy character are classified into two main classes according to the behavior of their zone-center optical phonons [7,8]. In the one-mode class, the frequencies vary continuously and approximately linearly with the molar fraction of the alloy. In the case of the two-mode behavior the two sets of optical modes correspond nearly to that of the two pure crystals AC or BC that compose the alloy. For the TMCs $In_xGa_{1-x}N$, $Al_xGa_{1-x}N$, and $Al_xIn_{1-x}N$ the one-mode behavior of the optical phonons has been clearly observed [4–6], in agreement with predictions of model calculations.

The III-N semiconductors have the hexagonal wurtzite structure as their natural crystalline structure, and exhibit highly unusual properties in III-V compound semiconductors. Since wurtzite crystals have a different unit-cell structure (i.e., four atoms per unit cell) as well as lower symmetry compared to their cubic zinc-blende counterparts, the phonon dynamics and electron-phonon (e-p) interaction in this kind of materials may be substantially different from those in crystals with cubic symmetry. As is well known, there are many more distinct phonon branches (nine optical and three acoustic modes), and the phonon modes are not purely longitudinal or transverse except for the [0001] direction [9]. However, the current understanding of the phonon dynamics and polaronic effects in wurtzite nitride semiconductors is very primitive, especially for the III-N TMCs.

Over the past years, there was a wide experimental and theoretical study of the e-p interaction in zinc-blende semiconductors [10–14]. The rich knowledge about their optical phonon modes, e-p interaction, polaronic states and electronic effective mass has accumulated

[a] e-mail: zwyan@imau.edu.cn

in bulk and heterostructure systems. In semiconductor heterostructures, the presence of interfaces breaks the isotropy in one or more spatial directions, leading to the mixing of the longitudinal and transverse vibration polarizations [11,14], and all of them have been included in the study of e-p interaction since the TO-like modes can provide a non-negligible contribution to the scattering rates and polaron properties. In recent years, the electron-optical phonon mode interaction mechanism in crystals with wurtzite structure has been considered. A new Fröhlich e-p interaction Hamiltonian was put forward for the bulk and heterostructures case [15–17], within the non retarded dielectric continuum model considering only the three optical-phonon branches (the one ordinary and two extraordinary optical phonons) which are infrared active in this crystal structure. Furthermore, the existence of a spatial direction with low symmetry (z-axis) also gives rise to phonon dispersion. For wurtzite nitrides the dependence of the extraordinary optical phonon frequencies upon the phonon wave-vector $\vec{q}$ is not a function of the wave-vector magnitude but of the angle θ between $\vec{q}$ and the c-axis of the structure (referred as the z direction in the following) [9]. Wurtzite nitrides are polar materials that exhibit stronger polaronic properties in comparison to the rest of III-V semiconductors, including a significant anisotropy effect in the polaronic effective mass [18,19]. Recently, the authors used a variational theory to study the intermediate-coupling polaron in wurtzite nitride semiconductors [20]. The results show that the structural anisotropy increases the e-p interaction due to the low-dimensionality effect. However, only few works, to our knowledge, have mentioned the e-p interaction in wurtzite III-N TMCs [19]. Further theoretical and experimental studies on the polaron effects are needed.

In the present paper, we study polaron properties in wurtzite III-N TMCs by using a variational treatment in the framework of the dielectric continuum model [20,21], by considering the anisotropy of the wurtzite structure. An effective polaron Hamiltonian for wurtzite III-N TMCs is obtained by using a Lee, Low and Pines (LLP)-like method [22,23] in Section 2. In Section 3, a variational calculation for the formulae of polaronic self-trapping energies, the e-p coupling constants and effective masses in wurtzite III-N TMCs are derived. Numerical results for the wurtzite TMC materials $In_xGa_{1-x}N$, $Al_xGa_{1-x}N$, and $Al_xIn_{1-x}N$ are given as functions of the composition x and discussed in Section 4.

2 Polaron Hamiltonian

Details of the optical phonon modes in the wurtzite III-N TMC $A_xB_{1-x}N$ can be found -in the MREI model [4,5]. It is found that optical phonons (A_1 and E_1) in $In_xGa_{1-x}N$, $Al_xGa_{1-x}N$, and $Al_xIn_{1-x}N$ exhibit one-mode behavior [4–6] unlike $Ga_xAl_{1-x}As$ and $In_xGa_{1-x}As$, which exhibit two-mode behavior [7,8]. In the one-mode case, the effect of the value of the composition x is introduced by assuming a linear dependence on this variable in the electron effective mass, the optical dielectric constant, and the fundamental phonon frequencies. Static dielectric constants are then obtained with the use of the Lyddane-Sachs-Teller relation. The ternary material parameters can be derived from binary parameters in linear interpolation by

$$T_{A_xB_{1-x}N}(x) = xT_{AN} + (1-x)T_{BN}. \tag{1}$$

We consider a uniaxial nitride semiconductor in which only one group of the three optical-phonon branches is infrared active in the Raman scatting. The wurtzite structure is a case in point since at the Γ point, only the $A_1(Z)$ and $E_1(X,Y)$ modes are infrared active among the nine optical phonon modes. We take the c-axis along the z direction and denote its perpendicular direction as $\perp$. Within the macroscopic dielectric continuum model and the uniaxial model, the e-p interaction Hamiltonial in the uniaxial crystals has been derived in recently [9,20]. Here, we only mention that it includes two terms: one corresponds to a LO-like e-p interaction, and the second to a TO-like interaction. The dispersion relations for both kinds of modes are function of the angle θ between the phonon wavevector $\vec{q}$ and the c-axis of the hexagonal lattice, but not of its magnitude. The Hamiltonian of such an e-p system can be written as [8,9,15–17,20]

$$\begin{aligned} H &= H_e + H_{ph} + H_{e-p} \\ &= \frac{p_\perp^2}{2m_\perp} + \frac{p_z^2}{2m_z} + \sum_{j\vec{q}} \hbar\omega_j a_{j\vec{q}}^+ a_{j\vec{q}} + \sum_{j\vec{q}} \left(G_{j\vec{q}}\, e^{i\vec{q}\cdot\vec{r}} a_{j\vec{q}} + \text{h.c.}\right), \end{aligned} \tag{2}$$

where $j(=L,T)$ is the mode-index of the phonon characteristic frequencies and

$$G_{j\vec{q}} = \left(\frac{e^2\hbar}{\varepsilon_0 V}\right)^{1/2} \frac{1}{q} \left(\frac{\partial \varepsilon_\theta^j}{\partial \omega_j}\right)^{-1/2}, \tag{3}$$

$$\frac{\partial \varepsilon_\theta^j}{\partial \omega_j} = \frac{\partial \varepsilon_\perp(\omega_j)}{\partial \omega_j} \sin^2\theta + \frac{\partial \varepsilon_z(\omega_j)}{\partial \omega_j} \cos^2\theta. \tag{4}$$

The dielectric functions of direction-dependent $\varepsilon_\perp(\omega)$ and $\varepsilon_z(\omega)$ are given by

$$\varepsilon_\perp(\omega) = \varepsilon_\perp^\infty \frac{\omega^2 - \omega_{\perp L}^2}{\omega^2 - \omega_{\perp T}^2}, \tag{5}$$

and

$$\varepsilon_z(\omega) = \varepsilon_z^\infty \frac{\omega^2 - \omega_{zL}^2}{\omega^2 - \omega_{zT}^2}, \tag{6}$$

$\varepsilon_\perp^\infty(\varepsilon_z^\infty)$ being the high-frequency dielectric constant perpendicular to (along) the z axis, and $\varepsilon_\perp^0 = \varepsilon_\perp^\infty \omega_{\perp L}^2/\varepsilon_{\perp T}^2$; $\varepsilon_z^0 = \varepsilon_z^\infty \omega_{zL}^2/\varepsilon_{zT}^2$ are the static dielectric constants. ω_{zL} and $\omega_{\perp L}$ are the LO-phonon frequencies along and perpendicular to the z axis, respectively, and ω_{zT} and $\omega_{\perp T}$ are the corresponding TO-phonon frequencies.

The phonon mode for extraordinary phonons are obtained from the phonon dispersion relation [9,15]:

$$\varepsilon_\theta^j(\omega) = \varepsilon_\perp(\omega)\sin^2\theta + \varepsilon_z(\omega)\cos^2\theta = 0. \tag{7}$$

$$
\begin{aligned}
H^* &= U_2^{-1}U_1^{-1}HU_1U_2 \\
&= \frac{1}{2m_\perp}\left(\vec{P}_\perp - \sum_{j\vec{q}} a^+_{j\vec{q}}a_{j\vec{q}}\hbar\vec{q}_\perp\right)^2 + \frac{1}{2m_z}\left(P_z - \sum_{j\vec{q}} a^+_{j\vec{q}}a_{j\vec{q}}\hbar q_z\right)^2 + \sum_{j\vec{q}}\hbar\omega_j a^+_{j\vec{q}}a_{j\vec{q}} \\
&\quad + \sum_{j\vec{q}}\left[G_{j\vec{q}}f_j(\vec{q}) + G^*_{j\vec{q}}f^*_j(\vec{q})\right] + \frac{\hbar^2}{2m_\perp}\left[\sum_{j\vec{q}}|f_j(\vec{q})|^2\vec{q}_\perp\right]^2 + \frac{\hbar^2}{2m_z}\left[\sum_{j\vec{q}}|f_j(\vec{q})|^2 q_z\right]^2 \\
&\quad + \sum_{j\vec{q}}|f_j(\vec{q})|^2\left(\hbar\omega_j - \frac{\hbar}{m_\perp}\vec{q}_\perp\cdot\vec{P}_\perp - \frac{\hbar}{m_z}q_zP_z + \frac{\hbar^2q_\perp^2}{2m_\perp} + \frac{\hbar^2q_z^2}{2m_z}\right) \\
&\quad + \frac{\hbar^2}{m_\perp}\sum_{j\vec{q}} a^+_{j\vec{q}}a_{j\vec{q}}\vec{q}_\perp\cdot\left[\sum_{j'\vec{q}'}\left|f_{j'}(\vec{q}')\right|^2\vec{q}'_\perp\right] + \frac{\hbar^2}{m_z}\sum_{j\vec{q}} a^+_{j\vec{q}}a_{j\vec{q}}q_z\left[\sum_{j'\vec{q}'}\left|f_{j'}(\vec{q}')\right|^2 q'_z\right] \\
&\quad + \sum_{j\vec{q}} a^+_{j\vec{q}}\left\{G^*_{j\vec{q}} + f_j(\vec{q})\left[\begin{array}{l}\hbar\omega_j - \dfrac{\hbar\vec{q}_\perp\cdot\vec{P}_\perp}{m_\perp} - \dfrac{\hbar q_zP_z}{m_z} + \dfrac{\hbar^2q_\perp^2}{2m_\perp} + \dfrac{\hbar^2q_z^2}{2m_z} \\ + \dfrac{\hbar}{m_\perp}\vec{q}_\perp\cdot\left(\sum\limits_{j'\vec{q}'}|f_{j'}(\vec{q})|^2\vec{q}'_\perp\right) + \dfrac{\hbar}{m_z}q_z\left(\sum\limits_{j'\vec{q}'}|f_{j'}(\vec{q})|^2 q'_z\right)\end{array}\right] + \text{h.c.}\right\},
\end{aligned}
\tag{12}
$$

We assume $\varepsilon_z^\infty = \varepsilon_\perp^\infty$; this quite a good assumption since ε^∞ is primarily due to electrons. Then,

$$
\frac{\omega^2-\omega_{\perp L}^2}{\omega^2-\omega_{\perp T}^2}\sin^2\theta + \frac{\omega^2-\omega_{zL}^2}{\omega^2-\omega_{zT}^2}\cos^2\theta = 0. \tag{8}
$$

When we have $|\omega_{\perp L}-\omega_{zL}|, |\omega_{\perp T}-\omega_{zT}| < |\omega_{\perp L}-\omega_{\perp T}|, |\omega_{zL}-\omega_{zT}|$, which is the case for the wurtzite-based III-V nitrides, the solutions are

$$
\omega_L^2 = \omega_{zL}^2\cos^2\theta + \omega_{\perp L}^2\sin^2\theta, \tag{9a}
$$

and

$$
\omega_T^2 = \omega_{zT}^2\sin^2\theta + \omega_{\perp T}^2\cos^2\theta. \tag{9b}
$$

These are the characteristic frequencies of predominantly LO-like and TO-like modes, respectively.

Now we extend the LLP method [22,23], which has been successfully used to solve the intermediate-coupling polaron problem in cubic (isotropic) polar crystals, to the present situation where the electron couples with both branches of LO-like and TO-like phonons. Making two unitary transformations as follows:

$$
U_1 = \exp\left(-i\sum_{j\vec{q}} a^+_{j\vec{q}}a_{j\vec{q}}(\vec{q}_\perp\cdot\vec{\rho} + q_zz)\right), \tag{10a}
$$

$$
U_2 = \exp\left\{\sum_{j\vec{q}}\left[a^+_{j\vec{q}}f_j(\vec{q}) - a_{j\vec{q}}f^*_j(\vec{q})\right]\right\}, \tag{10b}
$$

and introducing the total momentum operators

$$
\vec{P}_\perp = \vec{p}_\perp + \sum_{j\vec{q}}\hbar\vec{q}_\perp a^+_{j\vec{q}}a_{j\vec{q}}, \quad P_z = p_z + \sum_{j\vec{q}}\hbar q_z a^+_{j\vec{q}}a_{j\vec{q}}, \tag{11}
$$

the Hamiltonian can be transformed into the following form

see equation (12) above,

where higher order terms of $a^+_{j\vec{q}}$, $a_{j\vec{q}}$ have been neglected because they have no contribution to the expectation value for the zero phonon states. In the second unitary transformation, the displacement amplitudes $f_j(\vec{q})$ and $f^*_j(\vec{q})$ will be determined by minimizing the expectation value of the polaron energy as follows.

3 Variational method

As a first approximation, we confine our discussion on the low-temperature limit, i.e. the zero-phonon state of polaron. The expectation value of the polaron Hamiltonian (12) in the zero-phonon state $|0\rangle$ ($\langle 0 \mid 0\rangle = 1$) is given by

$$
\begin{aligned}
E(P) &= \langle 0|H^*|0\rangle \\
&= \frac{P_\perp^2}{2m_\perp} + \frac{P_z^2}{2m_z} + \sum_{j\vec{q}}\left[G_{j\vec{q}}f_j(\vec{q}) + G^*_{j\vec{q}}f^*_j(\vec{q})\right] \\
&\quad + \frac{\hbar^2}{2m_\perp}\left[\sum_{j\vec{q}}|f_j(\vec{q})|^2\vec{q}_\perp\right]^2 + \frac{\hbar^2}{2m_z}\left[\sum_{j\vec{q}}|f_j(\vec{q})|^2 q_z\right]^2 \\
&\quad + \sum_{j\vec{q}}\left(\hbar\omega_j - \frac{\hbar}{m_\perp}\vec{q}_\perp\cdot\vec{P}_\perp - \frac{\hbar}{m_z}q_zP_z + \frac{\hbar^2q_\perp^2}{2m_\perp} + \frac{\hbar^2q_z^2}{2m_z}\right)|f_j(\vec{q})|^2.
\end{aligned}
\tag{13}
$$

According to the variation principle, the necessary conditions to be satisfied by $f_j(\vec{q})$ and $f^*_j(\vec{q})$ are

$$
\frac{\partial E(\vec{P})}{\partial f_j(\vec{q})} = \frac{\partial E(\vec{P})}{\partial f^*_j(\vec{q})} = 0. \tag{14}
$$

We derive

$$G_{j\vec{q}} + f_j^*(\vec{q}) \times \left[\begin{array}{l} \left(\hbar\omega_j - \dfrac{\hbar}{m_\perp}\vec{q}_\perp \cdot \vec{P}_\perp - \dfrac{\hbar}{m_z} q_z \cdot P_z \right. \\ \qquad \left. + \dfrac{\hbar^2 q_\perp^2}{2m_\perp} + \dfrac{\hbar^2 q_z^2}{2m_z} \right) \\ + \dfrac{\hbar^2}{m_\perp} \sum\limits_{j\vec{q}'} \vec{q}'_\perp \cdot \vec{q}_\perp f_j(\vec{q}') + \dfrac{\hbar^2}{m_z} \sum\limits_{j\vec{q}'} q'_z q_z f_j(\vec{q}') \end{array} \right] = 0. \tag{15}$$

Let

$$\sum_{j\vec{q}} \hbar\vec{q} |f_j(\vec{q})|^2 = \eta \vec{P}, \tag{16}$$

where $\vec{P} = (\vec{P}_\perp, P_z)$ is the total momentum and $\vec{q} = (\vec{q}_\perp, q_z)$ is the phonon wave-vector. We have adopted $P_\perp = P\sin\beta$, $P_z = P\cos\beta$ and $q_\perp = q\sin\theta$, $q_z = q\cos\theta$. Here β is the angle between the total momentum $\vec{P}$ and the c-axis. Without loosing generality, $\vec{q}$, $\vec{P}$ and the c-axis can be assumed in the same plane. We solve (15) and obtain

$$f_j^*(\vec{q}) = - \frac{G_{j\vec{q}}}{\hbar\omega_j - \frac{\hbar\vec{q}_\perp \cdot \vec{P}_\perp}{m_\perp}(1-\eta) - \frac{\hbar q_z P_z}{m_z}(1-\eta) + \frac{\hbar^2 q_\perp^2}{2m_\perp} + \frac{\hbar^2 q_z^2}{2m_z}}. \tag{17}$$

Inserting equation (17) in (16), we obtain

$$\eta P^2 = \sum_{j\vec{q}} \frac{2\left|G_{j\vec{q}}\right|^2 \hbar^2 (qP)^2 D(1-\eta)\cos(\beta-\theta)}{\left(\hbar\omega_j + \frac{\hbar^2 q^2}{2m}\right)^3}. \tag{18}$$

It gives

$$\eta = \frac{A}{1+A}, \tag{19}$$

where

$$\begin{aligned} D &= \frac{1}{m_\perp}\sin\theta\sin\beta + \frac{1}{m_z}\cos\theta\cos\beta, \\ A &= \sum_{j\vec{q}} \frac{2\left|G_{j\vec{q}}\right|^2 \hbar^2 q^2 D\cos(\beta-\theta)}{\left(\hbar\omega_j + \frac{\hbar^2 q^2}{2m}\right)^3}, \\ \frac{1}{m} &= \frac{\sin^2\theta}{m_\perp} + \frac{\cos^2\theta}{m_z}. \end{aligned} \tag{20}$$

Then inserting equations (17)–(20) into (13), we finally obtain the energy of the zero-phonon state of the polaron as follows

$$\begin{aligned} E(\vec{P}) &= \frac{P^2}{2m^*} - E_{tr} \\ &= \frac{P^2}{2m^*} - \sum_{j\vec{q}} \frac{\left|G_{j\vec{q}}\right|^2}{\hbar\omega_j + \frac{\hbar^2 q^2}{2m}} + O(P^4), \quad j = L, T \end{aligned} \tag{21}$$

The last term in equation (21) stands for the higher order terms over fourth power of the total momentum $\vec{P}$, which can be neglected for slow-moving polarons. m^* is the polaron effective mass and can be given by

$$m^* = m'\left(1 + \sum_j \Delta m_j\right). \tag{22}$$

$$E_{tr} = E_{tr}^L + E_{tr}^T = \sum_{\vec{q}} \frac{\left|G_{L\vec{q}}\right|^2}{\hbar\omega_L + \frac{\hbar^2 q^2}{2m}} + \sum_{\vec{q}} \frac{\left|G_{T\vec{q}}\right|^2}{\hbar\omega_T + \frac{\hbar^2 q^2}{2m}}. \tag{23}$$

Here E_{tr}^L and E_{tr}^T are, respectively, the contributions of the LO-like and TO-like phonons to the polaron self-trapping energy. Δm_L and Δm_T are related respectively to LO-like and TO-like phonons and defined as follows

$$\Delta m_j = \frac{A^2 + B}{1 + 2A - B}, \tag{24}$$

where

$$B = \sum_{j\vec{q}} \frac{2m' \left|G_{j\vec{q}}\right|^2 q^2 D^2}{\left(\hbar\omega_j + \frac{\hbar^2 q^2}{2m}\right)^3}, \quad m' = \frac{m_\perp m_z}{m_\perp \cos^2\beta + m_z \sin^2\beta}. \tag{25}$$

Changing the summation in the above equations into an integration by using the following relation

$$\sum_{\vec{q}} \to \frac{V}{(2\pi)^3}\int d\vec{q}, \tag{26}$$

the polaronic self-trapping energy can be rewritten as

$$\begin{aligned} E_{tr} &= E_{tr}^L + E_{tr}^T = \sum_{j\vec{q}} \alpha_j(\vec{q})\hbar\omega_j \\ &= \sum_{j=L,T} \frac{e^2}{8\pi\varepsilon_0}(2m)^{1/2} \int_0^\pi \left(\frac{1}{\hbar\omega_j}\right)^{1/2} \left(\frac{\partial\varepsilon_\theta^j}{\partial\omega_j}\right)^{-1} \sin\theta d\theta. \end{aligned} \tag{27}$$

An effective e-p coupling constant α is introduced to describe the total effect of the e-p interaction on the polaronic self-trapping energy, and it can be written as

$$\begin{aligned} \alpha &= \alpha_L + \alpha_T = \sum_{j\vec{q}} \alpha_j(\vec{q}) \\ &= \sum_{j=L,T} \frac{e^2}{8\pi\varepsilon_0}(2m)^{1/2} \int_0^\pi \left(\frac{1}{\hbar\omega_j}\right)^{3/2} \left(\frac{\partial\varepsilon_\theta^j}{\partial\omega_j}\right)^{-1} \sin\theta d\theta. \end{aligned} \tag{28}$$

In a similar way in equation (24), one can obtain the influence of phonons on the polaronic effective mass Δm_L and Δm_T. The complexity of equations (24, 25) needs numerical solution.

Table 1. Parameters used in the calculation. Energy is measured in meV and mass in electron rest mass m_0.

Materials	A_1(TO)	A_1(LO)	E_1(TO)	E_1(LO)	ε_z^0	$\varepsilon_\perp^0$	$\varepsilon_z^\infty = \varepsilon_\perp^\infty$	m_z	$m_\perp$
	ω_{zT}	ω_{zL}	$\omega_{\perp T}$	$\omega_{\perp L}$					
GaN	66.06	91.10	69.53	91.97	10.18	9.36	5.35	0.20	0.20
AlN	71.10	110.68	83.42	113.54	11.72	8.97	4.84	0.32	0.28
InN	54.91	72.63	57.88	73.75	14.70	13.64	8.4	0.12	0.12

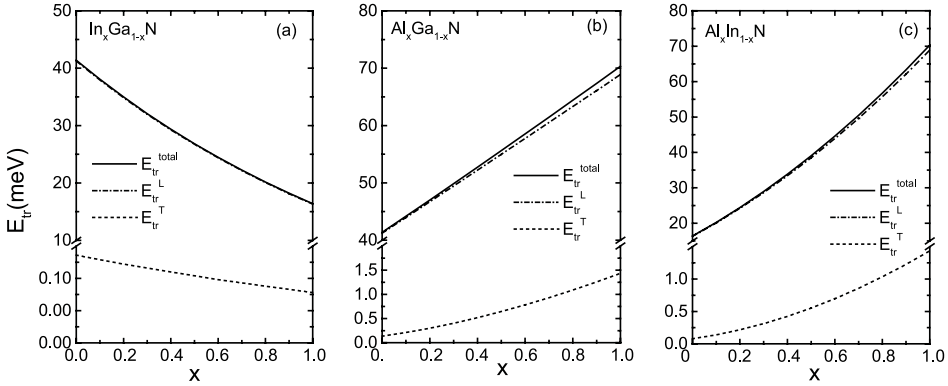

Fig. 1. Polaron self-trapping energies E_{tr} as functions of the composition x for several wurtzite TMCs of III-N compounds: (a) $In_xGa_{1-x}N$, (b) $Al_xGa_{1-x}N$ and (c) $Al_xIn_{1-x}N$.

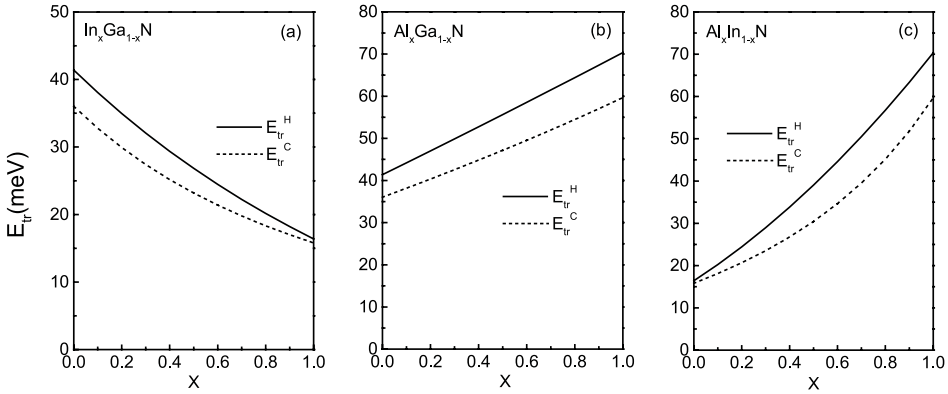

Fig. 2. Polaron self-trapping energies E_{tr} for wurtzite (solid lines) and zinc-blende (dashed lines) alloys as functions of the composition x for several TMCs of III-N compounds: (a) $In_xGa_{1-x}N$, (b) $Al_xGa_{1-x}N$ and (c) $Al_xIn_{1-x}N$.

4 Numerical results and discussion

We have numerically computed the self-trapping energies, e-p coupling constants and effective masses of the polarons in $In_xGa_{1-x}N$, $Al_xGa_{1-x}N$, and $Al_xIn_{1-x}N$. The parameters used in the computation are listed in Table 1 [3,24] for binary wurtzite III-N semiconductor materials, and the results are illustrated and discussed in Figures 1–4.

Figure 1 shows the polaronic self-trapping energies as functions of the composition x for $In_xGa_{1-x}N$, $Al_xGa_{1-x}N$, and $Al_xIn_{1-x}N$ materials. It is clearly seen from Figure 1 that the self-trapping energies as functions of the composition x are monotonous, and are nonlinear for $In_xGa_{1-x}N$ and $Al_xIn_{1-x}N$ and almost linear for $Al_xGa_{1-x}N$. The self-trapping energies due to the e-p interaction are, in fact, rather significant. It follows that the stronger the e-p coupling or broad forbidden energy gaps (EFGs) are, the greater are the self-trapping energies. It is found that the contribution from the TO-like modes is approximately two orders magnitude smaller than the LO-like. As expected, the main contribution comes from the LO-like modes. We can obtain the values corresponding to the end materials at $x = 0$ and $x = 1$: $E_{tr} = E_{tr}^L + E_{tr}^T = 41.39$ meV for GaN, =70.32 meV for AlN, 16.66 meV for InN, respectively, in agreement with previous calculations [20]. Furthermore, the zinc-blende phase in III-N TMCs has been found a few years ago [8,19,23]. For the sake of comparison, we have also calculated the polaronic self-trapping energies for zinc-blende structures of the above three materials using a variational approach [22]. The self-trapping energy of hexagonal wurtzite (E_{tr}^H) and cubic zinc-blende (E_{tr}^C) structures are plotted as functions of x in direct comparison in Figure 2. It can easily be seen that the wurtzite structures E_{tr}^H

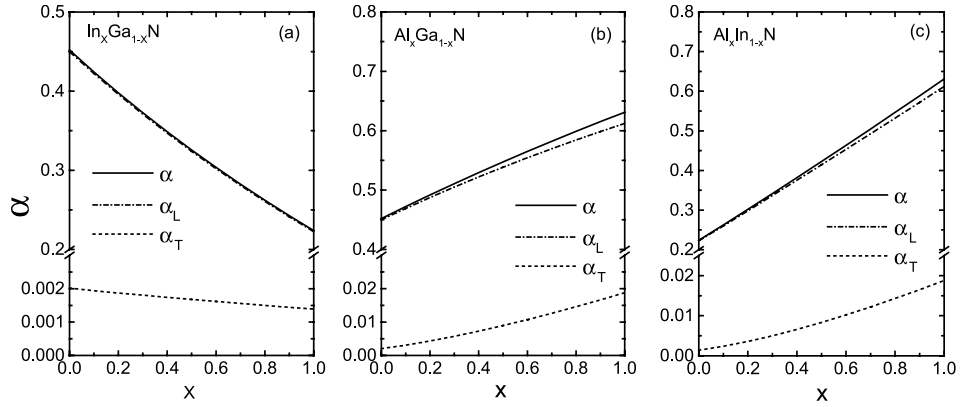

Fig. 3. The effective e-p interaction coupling constants α as functions of the composition x for several wurtzite TMCs of III-N compounds: (a) $In_xGa_{1-x}N$, (b) $Al_xGa_{1-x}N$ and (c) $Al_xIn_{1-x}N$.

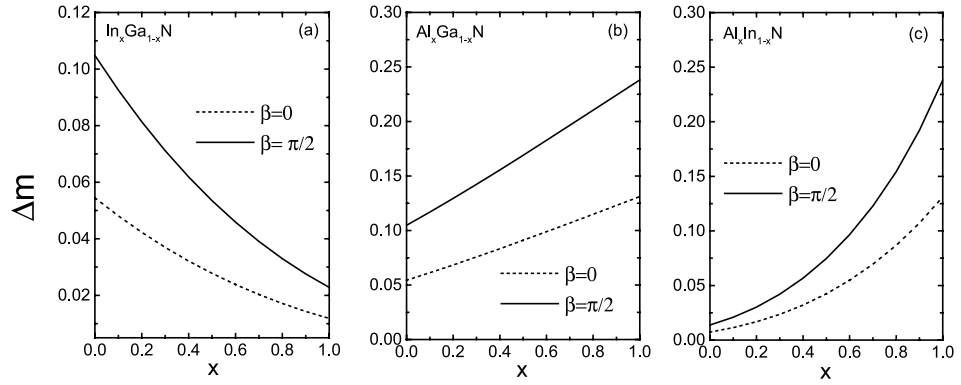

Fig. 4. Phonon contributions to the polaron effective masses Δm as functions of the composition x for several wurtzite TMCs of III-N compounds: (a) $In_xGa_{1-x}N$, (b) $Al_xGa_{1-x}N$ and (c) $Al_xIn_{1-x}N$.

are bigger than the zinc-blende materials E_{tr}^C in the entire regions of composition x. These incremental values $\Delta E_{tr} = E_{tr}^H - E_{tr}^C$ are also related to the width of the FEG. It can be seen in Figure 2 that the broader FEG generally causes the greater ΔE_{tr} for the self-trapping energies of the above calculated materials. At the end of $x = 0$ and $x = 1$, the TMC reduces to the binary crystals AN and BN. The net incremental values ΔE_{tr} are 5.35 meV, 10.56 meV, and 2.18 meV for GaN, AlN and InN, respectively. The self-trapping energies exhibit an anisotropy with about 15% (for GaN), 17.6% (for AlN), and 10.1% (for InN). For the wurtzite III-N TMC materials, the calculational results also show that the structure anisotropy increases the e-p interaction due to the low-dimensionality effect. This verifies important conclusion: the polaronic self-trapping in two dimensions is deeper than that in three dimensions.

To clearly understand the intensity of the e-p coupling effects in the wurtzite III-N TMCs, the effective e-p coupling constants α as functions of the composition x are illustrated in Figure 3. It is seen that there are monotonous changes (almost linear) with compositions x for $In_xGa_{1-x}N$, $Al_xGa_{1-x}N$, and $Al_xIn_{1-x}N$ materials. It is found that the magnitude of the electron- LO-like phonon coupling constants α_L is approximately two orders bigger than the TO-like α_T for these materials. It is also shown that the effective e-p coupling constants α are less than unity in the entire range of composition x, and are stronger than those for usual III-V group TMC materials like $Ga_xAl_{1-x}As$ and $In_xGa_{1-x}As$. We also computed the binary crystals for wurtzite nitrides GaN, AlN and InN, and the results are: $\alpha = 0.452$ for GaN, 0.631 for AlN, 0.224 for InN, respectively. We can conclude that the polaron problem for wurzite (hexagonal symmetry) nitride semiconductors can be dealt with intermediate coupling approach, which may give more accurate results and work well in a larger range of the band gap width.

Figure 4 gives the relative shift of the polaronic effective mass Δm due to the influence of phonons as functions of the compositions x for the above three wurtzite nitride TMC materials. It is clearly seen from Figure 4 that the characteristics of the curves of $\beta = \pi/2$ and $\beta = 0$ are similar for the materials computed, where β is the angle between the total momentum $\vec{P}$ and the c-axis. The magnitudes of the phonon influence on the effective mass are always monotonically increasing with the FEG width. It is found that Δm for $\beta = \pi/2$ is bigger than for $\beta = 0$. It follows that the contribution variations of phonons to the relative shift of the polaronic effective mass become bigger from $\beta = 0$ to $\beta = \pi/2$ when the FEG becomes wider, for example, $\Delta m^*(\pi/2) - \Delta m^*(0) = 0.051$ (for GaN), 0.117 (for AlN), and 0.011 (for InN), respectively. The stronger

the e-p coupling or broader the FEG, the greater is the anisotropy influence on the polaronic effective mass for $In_xGa_{1-x}N$, $Al_xGa_{1-x}N$, and $Al_xIn_{1-x}N$. The anisotropy in the polaronic effective mass due to the phonon influence is shown to be significant as well, for the three wurtzite III-N TMCs materials, and cannot be neglected. It should be pointed out that the magnitude of the polaronic effective mass is also related to some other material factors such as the phonon frequencies and dielectric constants. It makes the anisotropy effect more complicated. We also calculated the contributions from LO-like phonons and TO-like on effective mass as functions of the compositions x for $In_xGa_{1-x}N$, $Al_xGa_{1-x}N$, and $Al_xIn_{1-x}N$. It is indicated that the LO-like phonons influence on polaronic effective mass is always larger approximately two orders of magnitude than that from TO-like phonons over the range of compositions x. This conclusion is in agreement with our previous work [20]. It shows that the TO-like phonon influence on the polaron effective mass is unimportant.

In summary, a variational method has been developed to calculate the self-trapping energies and effective masses of polarons in wurtzite (hexagonal structure) III-N TMCs. The anisotropy effect on the polarons in wurtzite III-N TMCs is obtained and discussed for materials $In_xGa_{1-x}N$, $Al_xGa_{1-x}N$, and $Al_xIn_{1-x}N$. The numerical results show that the structure anisotropy increases the e-p interaction due to the low-dimensionality effect. It indicates that the anisotropy effect on the polaronic self-trapping energy and effective mass is obvious. It is also found that the polaronic self-trapping energy and effective mass increase with the FEG width. The results show that the LO-like phonon influence on the polaronic self-trapping energy and effective mass is dominant.

The work was supported by the National Natural Science Foundation of P.R. China (Project 10264003) and the Educational Science Foundation of Inner Mongolia Autonomous Region of P.R. China (Project NJ02054) and Project for Excellence Subject-Director of Inner Mongolia Autonomous Region of P.R. China.

References

1. S. Nakamura, *The Blue Laser Diode-GaN Based Light Emitters and Lasers* (Springer, Berlin, 1997)
2. S. Strite, H. Morkoc, J. Vac. Sci. Technol. B **10**, 1237 (1992)
3. C. Bungaro, K. Rapcewicz, J. Bernholc, Phys. Rev. B **61**, 6720 (2000)
4. S.G. Yu, K.W. Kim, L. Bergman, M. Dutta, M.A. Stroscio, M. Zavada, Phys. Rev. B **58**, 15283 (1998)
5. H. Grille, C. Schnittler, F. Bechstedt, Phys. Rev. B **61**, 6091 (2000)
6. A. Kasic, M. Schubert, J. Off, F. Scholz, Appl. Phys. Lett. **78**, 1256 (2001)
7. I.F. Chang, S.S. Mitria, Adv, Phys. **20**, 359 (1971)
8. X.X. Liang, S.L. Ban, Chinese Physics **13**, 71 (2004)
9. R. Loudon, Adv. Phys. **13**, 423 (1996); W. Hayes, R. Loudon, *Scatting of Light by Crystals* (Wiley, New York, 1978)
10. J.T. Devreese, *Polarons in Ionic Crystals and Polar Semiconductors* (North-Holland, Amsterdam, 1972)
11. N. Mori, T. Ando, Phys. Rev. B **40**, 6175 (1989)
12. Z.W. Yan, S.L. Ban, X.X. Liang, Eur. Phys. J. B **35**, 41 (2003)
13. F.M. Peeters, J.T. Devreese, Phys. Rev. B **36**, 4442 (1987)
14. J.E. Zucker, A. Pinczuk, D.S. Chemla, A. Gossard, W. Wiegmann, Phys. Rev. Lett. **53**, 1280 (1984)
15. B.C. Lee, K.W. Kim, M. Dutta, M.A. Stroscio, Phys. Rev. B **56**, 997 (1997)
16. E.R. Racec, D.E.N. Brancus, J. Phys. C **10**, 3857 (1998)
17. J.J. Shi, Phys. Rev. B **68**, 165335 (2003)
18. M.E. Mora-Ramos, F.J. Rodríguez, L. Quiroga, Phys. Stat. Sol. (b) **220**, 111 (2000), Solid State Commun. **109**, 767 (1999)
19. M.E. Mora-Ramos, Phys. Stat. Sol. (b) **223**, 843 (2001)
20. Z.W. Yan, S.L. Ban, X.X. Liang, Phys. Lett. A **236**, 157 (2004)
21. M. Born, K. Huang, *Dynamical Theory of Crystal Lattices* (Clarendon Press, Oxford, England, 1954)
22. T.D. Lee, F.E. Low, D. Pines, Phys. Rev. **90**, 297 (1953)
23. X.X. Liang, Y.S. Zhang, Z. Phys. B **91**, 455 (1993)
24. I. Vurgaftman, I.R. Ram-Mohan, J. Appl. Phys. **89**, 5815 (2001)